Available online at www.sciencedirect.com
ScienceDirect
Chaos, Solitons and Fractals 39 (2009) 1210–1223
CHAOS
SOLITONS & FRACTALS
www.elsevier.com/locate/chaos

Strength vs. toughness optimization of microstructured composites

Alberto Carpinteri *, Nicola Pugno, Simone Puzzi

Department of Structural Engineering and Geotechnics, Politecnico di Torino, Corso Duca degli Abruzzi 24, 10129 Torino, Italy

Accepted 25 May 2007

Abstract

Aim of this paper is to present a new fractal approach linking the macroscopic mechanical properties of micro- and nano-structured materials with the main parameters: composition, grain size and structural dimension, as well as contiguity and mean free path. Assuming the key role played by the interfaces, the proposed fractal energy approach unifies the influences of all the above parameters, through the introduction of a fractal structural parameter (FSP), which represents an extension of the Gurland's structural parameter. This modeling approach is assessed through an extensive comparison with experimental data on poly crystalline diamond (PCD) and WC–Co alloys. The results clearly show that the theoretical fractal predictions are in a fairly good agreement with the experiments on both hardness and toughness. This new synthetic parameter is thus proposed to investigate, design and optimize new micro- and nano-grained materials. Eventually, FSP-based optimization maps are developed, that allow to design new materials with high hardness and toughness.
© 2007 Elsevier Ltd. All rights reserved.

1. Introduction

Composites consisting of a brittle hard material, whether ceramic or intermetallic, reinforced with a ductile phase, are very important in several industrial applications, due to their mechanical properties, which include high hardness, wear resistance and toughness. From an experimental point of view, a direct relationship between the fabrication process, the microstructure and the properties of these materials has been evidenced [1–3]). In the Literature several approaches, experimental, numerical and theoretical, have been proposed to correlate the macroscopic properties with the material microstructure, but a general theory for the dependence of hardness and toughness of composites such as WC–Co alloy or poly-crystalline diamond (PCD) on microstructural parameters has not been presented yet. In particular, tungsten carbide cobalt (WC–Co) alloys, due to their importance in industrial applications, have been investigated in great detail by several authors, who analysed the microstructural details and tried to pinpoint the most important parameters affecting the macroscopic properties [4–14]. Several

* Corresponding author. Tel.: +39 011 564 4850; fax: +39 011 564 4899.
E-mail address: alberto.carpinteri@polito.it (A. Carpinteri).
URL: http://staff.polito.it/alberto.carpinteri (A. Carpinteri).

0960-0779/$ - see front matter © 2007 Elsevier Ltd. All rights reserved.
doi:10.1016/j.chaos.2007.05.021

Nomenclature

C	contiguity
D	fractal exponent
d	mean grain size
d_r	reference grain size
H	hardness
h	mean free path
K_{IC}	toughness
l	characteristic crack length
N_0	number of grains
$p(\cdot)$	probability density function
R	structural size
r	grain size
r_{min}	minimum grain size
r_{max}	maximum grain size
S_g	total grain surface
V	volume
V_g	total grain volume
v	volumetric fraction of grains
v_r	reference volumetric fraction of grains
W	total dissipated energy
W_c	dissipated energy per unit volume
α	scaling exponent
γ	fractal exponent
k_σ	model parameter
k_K	model parameter
$k_{K\sigma}$	model parameter
σ_c	strength

different approaches have been proposed for modeling both hardness (or strength) and toughness of these materials, aiming at tailoring the mechanical properties of the composite materials by controlling the microstructure all along the fabrication process [15–21].

Regarding WC–Co alloys, the relation between fracture strength (and fracture toughness) and microstructure is a very attracting question, since experiments have clearly shown that these properties depend not only on the mean grain size d of WC but also on its volume fraction v, the mean free path h of the Co binder and the contiguity C of WC particles [15,16]. The choice of the independent parameters is still not clear and matter of research, particularly regarding the role of contiguity [20]. In their pioneering paper, Lee and Gurland [16] first pointed out the role of contiguity C and concluded that this parameter could not be left out in any modeling attempt, whilst more recently Makhele-Lekala et al. [20] explicitly aimed at the derivation of an empirical formula relating hardness to WC grain size d and mean free path h of Co, without explicit inclusion of contiguity. A similar result was obtained by Liu et al. [22] on the basis of a micromechanical model for polycrystalline aggregates with annular flaws surrounding the grains. Golovchan and Litoshenko [23] strengthened the view which considers contiguity not as a fundamental parameter, evidencing a dependency of C on the coefficient of variation of the WC grain size, whilst Armstrong and Cazacu [21] again include it in their analysis. The role of Cobalt mean free path h in controlling the fracture toughness of WC–Co alloys, first pointed out by Sigl and Fischmeister [24], is also not completely understood.

In spite of the large number of theoretical and experimental investigations, a unified approach to the strength and toughness of these materials is at its early stages [25]. Aim of this paper is the generalization and unification of the influences of the effects of all the above parameters, for both strength and toughness. In addition, the proposed model will also include the effect of the structural dimension R [26], that will be defined later. It is worthwhile noting that in the fractal model, that we are going to present, the mean free path h of the Co binder and the contiguity C of WC particles are not included directly, since their effects are implicitly taken into account by the proposed fractal structural parameter.

2. Composition, contiguity, grain size, mean free path and structural size

The effect of *composition* can be taken into account by means of mixture rules. Within these rules, the mechanical behaviour of the mixture is usually assumed to be independent of the grain and structural sizes. On the other hand, this result is clearly an oversimplification, as experiments demonstrate. Even if more sophisticated estimates of the overall tensor mechanical properties of heterogeneous solids and a comparison with the most common rules of mixture have been recently proposed [27,28], a clear understanding of the phenomenon is still absent in the literature.

Nevertheless, indicating with σ_c the strength of a micro- or nano-structured material, which is composed by a matrix having strength $\sigma_c^{\langle \text{matrix} \rangle}$ and grains with volumetric fraction v and strength $\sigma_c^{\langle \text{grain} \rangle}$, the simplest rule of mixture (direct rule) would predict:

$$\sigma_c = (1 - v)\sigma_c^{\langle \text{matrix} \rangle} + v\sigma_c^{\langle \text{grain} \rangle}. \tag{1}$$

A similar mixture rule may also be written for the fracture toughness K_{IC}:

$$K_{IC} = (1 - v)K_{IC}^{\langle \text{matrix} \rangle} + vK_{IC}^{\langle \text{grain} \rangle}. \tag{2}$$

The role of contiguity C, which is defined, according to Gurland [15], as *the average fraction of surface area shared by a grain with all neighbouring particles of the same phase*, may be taken into account by simply substituting the real volume fraction v of each phase with its *continuous fraction* $v^{(C)}$, that can be evaluated through the contiguity C as

$$v^{(C)} = vC. \tag{3}$$

As a consequence, the role of the contiguity can be simply considered substituting in the rules of mixture, at the place of the real volume fraction v, the effective one $v^{(C)}$ [16]. This approach is still popular and re-proposed also in the paper by Armstrong and Cazacu [21], although it is quite clear that the contiguity is not an independent parameter [23], since it depends on d and v, see Appendix A.

The effect of the *grain size* may also play a considerable role. As the grain size decreases, there is a significant increase in the volume fraction of grain boundaries or interfaces. This characteristic strongly influences the chemical and physical properties of the material. In materials that are conventionally quite strong but very brittle, such as intermetallic compounds and ceramics, grain size reduction enhances ductility through the increased probability of grain boundary sliding, offering considerable processing advantage and performance improvements. In the case of metals, on the other hand, the decrease in grain size may bring to significant increases in yield strength and elastic modulus, through the introduction of additional grain boundaries that can act as effective barriers to dislocation motion. This effect is usually described by means of the well-known Hall–Petch law [29,30]:

$$\sigma_c - k \propto d^{-1/2}, \tag{4}$$

where d is the mean grain size (and k is a constant).

The effect of the Co *mean free path* h on strength is again of the Hall–Petch type and similar to that reported in Eq. (4) if d is replaced by h [16]. Its effect on the fracture toughness is less clear and various dependencies of K_{IC} on h have been proposed: according to Ravichandran [19], $K_{IC} - k\prime \propto h$ ($k'$is a constant), whilst Armstrong and Cazacu [21] propose a dependence of the form: $K_{IC} - k\prime \propto h^{1/2}$. This uncertainty will be overcome in the forthcoming treatment, in which the effect of the mean free path is not considered, since this variable depends on the volume fraction v of hard phase and on the grain size d.

The effect of all these parameters are usually dealt with in a cascade-like approach [16,21]. In the case of hardness (or strength), for instance, first a mixture rule of the type of Eq. (1) is written, then the effects of grain size d and mean free path h are included by replacing $\sigma_c^{\langle \text{matrix} \rangle}$ and $\sigma_c^{\langle \text{grain} \rangle}$ with Hall–Petch empirical relationships (see Eq. (4)). The effect of contiguity C may be taken into account by replacing the volume fraction with the continuous volume fraction $v^{(C)}$ of Eq. (3), as already stated.

Regarding the *structural size* R, which is a characteristic length of the structure (e.g. the beam height in a three-point bending specimen, or the diameter in a cylindrical specimen), there is a large literature on its effect, which is usually called the *size-scale effect*. Dealing specifically with grained materials, it has been found experimentally that strength decreases with the structural size, whereas fracture energy increases [31,32]). All these effects will be included in the fractal treatment, that we are going to present.

3. Energy scaling

In order to predict the influence of grain size, structural dimension and composition (volumetric grain content) in a unified manner, a fractal approach is herein considered. Contiguity and mean free path are considered dependent parameters. Accordingly, we assume a fractal (or self-similar) distribution of reinforcement grains, for which the probability density function $p(r)$, describing their distribution in size r in the range $[r_{\min}, r_{\max}]$ has to be written as [33–35]:

$$p(r) = \frac{D}{1 - \left(\frac{r_{\max}}{r_{\min}}\right)^{-D}} \frac{r_{\min}^D}{r^{D+1}} \cong D \frac{r_{\min}^D}{r^{D+1}} \tag{5}$$

where $2 \leqslant D = 3\gamma \leqslant 3$ is the fractal exponent, $r_{\min}$ is the size of the smallest grain and $r_{\max}$ that of the largest grain. Notice that we assume $r_{\min} \ll r_{\max}$, so that the first denominator in the previous equation is very close to unity and the above approximation is justified. On the other hand, different types of grain size distribution can be considered as limit cases of the fractal approach, as discussed for the Gaussian by Carpinteri and Pugno [25].

The main assumption of the theory is that energy dissipation due to the presence of the reinforcement phase occurs only at the interfaces. It consists of different phenomena, such as constrained deformation of the matrix between grains, plasticity and fracture propagation. In particular we assume that the energy dissipation W, connected to the presence of the grains, is statistically expected to be proportional to their total surface area S_g [33], i.e.:

$$W \propto S_g \propto \int_{r_{\min}}^{r_{\max}} r^2 \mathrm{d}N \propto \int_{r_{\min}}^{r_{\max}} N_0 r^2 p(r) \mathrm{d}r \propto N_0 r_{\min}^2, \tag{6}$$

where $r_{\max}$ is the size of the largest grain and N_0 is the total number of grains. On the other hand, the total volume V_g of the grains is

$$V_g \propto \int_{r_{\min}}^{r_{\max}} r^3 \mathrm{d}N \propto \int_{r_{\min}}^{r_{\max}} N_0 r^3 p(r) \mathrm{d}r \propto N_0 r_{\min}^D r_{\max}^{3-D}. \tag{7}$$

Notice that both equations are obtained under the assumption that $r_{\min} \ll r_{\max}$. Deriving the expression of N_0 from the previous equation and putting it into Eq. (6), yields:

$$W \propto V_g r_{\min}^{2-D} r_{\max}^{D-3}. \tag{8}$$

As a consequence, the energy dissipated in the grains per unit volume V of the specimen becomes:

$$W_C = \frac{W}{V} \propto v r_{\min}^{2-D} r_{\max}^{D-3}, \tag{9}$$

where $v = V_g/V$ represents the volumetric fraction of the grains. Assuming the statistical self-similarity hypothesis, i.e., $r_{\max} \propto \sqrt[3]{V_g}$ (the larger the total volume of grains, the larger the largest grain), the effect of the structural size (size effect) can be obtained as

$$W_C \propto v r_{\min}^{2-D} V_g^{\frac{D-3}{3}}. \tag{10}$$

Usually $r_{\min}$ is assumed to be a constant, i.e., a material property. The mean value of the external surface of grains, proportional to $\langle r^2 \rangle$, as well as of their volume, proportional to $\langle r^3 \rangle$, are substantially estimated in Eqs. (6) and (7). On the other hand, the evaluation for the mean value of the grain size r gives:

$$\langle r \rangle \propto \frac{1}{N_0} \int_{r_{\min}}^{r_{\max}} r \mathrm{d}N \propto \int_{r_{\min}}^{r_{\max}} r p(r) \mathrm{d}r \propto r_{\min} \tag{11}$$

Introducing $D = 3\gamma$ and Eq. (11) into Eq. (10), noting that $V \approx R^3$ with R structural size, and $d \approx \langle r \rangle$ being the grain size, we can write:

$$W_C \propto v^{\gamma} d^{2-3\gamma} R^{3(\gamma-1)}, \tag{12}$$

that represents the scaling law of the additional energy density dissipated as a consequence of the presence of the grains and interfaces. It is worthwhile noting that this relation implicitly considers the grains embedded in the matrix; as a consequence, this energy density is not intrinsic to the grains only, but to the grains in the matrix. Eq. (12) is of great importance to predict the increment in strength due to the presence of grains, as discussed below. It is also noticeable that this result is consistent with findings by Carpinteri and Pugno [33–35] from fragmentation theories, see Appendix C.

4. Grain and structural size effects

According to the fractal approach, the relationship of Eq. (12) represents the unified law to evaluate the grain and structural size-effects, as well as the influence of composition, on the dissipated energy density. Let us focus our attention onto a structure of size R, constituted by a two-phase material, with only one grained phase of mean grain size d and volumetric percentage v. Noting that the square root of the dissipated energy due to the presence of the grains per unit specimen volume (if we assume negligible size-effects on the elastic modulus) can be considered to be proportional to the strength of the grains (not intrinsic, but in the matrix), and coupling Eq. (12) with a classical rule of mixture gives the following unified scaling law:

$$\sigma_c = (1-v)\sigma_c^{\langle \text{matrix} \rangle} + v\sigma_c^{\langle \text{grain} \rangle}, \tag{13a}$$

$$\sigma_c^{\langle \text{grain} \rangle} \approx k_\sigma v^{\frac{\gamma}{2}} R^{\frac{3}{2}(\gamma-1)} d^{1-\frac{3}{2}\gamma}, \tag{13b}$$

where k_σ is a constant and $\sigma_c^{\langle \text{matrix} \rangle}$ is the strength of the matrix. It is interesting to observe that, considering self-similar structures with the same scaling for the grain sizes, i.e., $d \propto R$, $v = \text{const.}$, the size effect on strength does not vanish – see Eq. (13):

$$\sigma_c \propto R^{-\frac{1}{2}}, \tag{14}$$

if we assume that the second term in Eq. (13a) is the dominating one. On the other hand, the exponent γ disappears. This seems to suggest that the size-effect of Eq. (14) is intrinsic, whereas the change of the exponents in the scaling laws (''geometrical'' multifractality) is a consequence of the competition between the grain size and the structural dimension, as demonstrated by means of a statistical approach by Carpinteri et al. [36,37].

The developed fractal theory unifies the grain and structural size effects and is in agreement with well-known size-effect laws [25], as well as with the Hall–Petch relationship ($\gamma = 1$; note that this corresponds to different grain size distributions, such as Gaussian [25], see Appendix B). We also note that Eq. (13) represent an extension of the Gurland [15] structural parameter, defined as

$$\sigma_c \propto k + v^{\frac{1}{3}} d^{-\frac{1}{2}} \tag{15}$$

and more generally an extension – including the volumetric content – of the Hall–Petch relationship [25]. For the hardness (or for the wear resistance) the same scaling of Eq. (13) is expected since:

$$H \propto \sigma_c. \tag{16}$$

The relationship analogous to the Hall–Petch law, has been experimentally confirmed for the hardness H, as an empirical law [15,16] for carbon-based materials, in agreement with the scaling of Eq. (13b).

An approximated law also can be proposed for the fracture toughness, with respect to the size and the volumetric content of grains. According to Griffith, if the characteristic crack length is l, $K_{IC}^{\langle \text{grain} \rangle} \propto \sigma_c^{\langle \text{grain} \rangle}\sqrt{l}$. Two plausible hypotheses for l are $l \propto R$ or $l \propto d$; thus, in general, we assume $l \propto d^{1-2\alpha}R^{2\alpha}$ where $\alpha, 0 < 2\alpha < 1$, is a constant. Accordingly, a classical rule of mixture yields:

$$K_{IC} \approx (1-v)K_{IC}^{\langle \text{matrix} \rangle} + vK_{IC}^{\langle \text{grain} \rangle}, \tag{17a}$$

$$K_{IC}^{\langle \text{grain} \rangle} \approx k_K \sigma_c^{\langle \text{grain} \rangle} d^{1/2-\alpha} R^{\alpha}, \tag{17b}$$

where k_K is a constant and $K_{IC}^{\langle \text{matrix} \rangle}$ is the fracture toughness of the matrix.

5. Fractal structural parameter and deviations from the empirical Hall–Petch law

The predictions of the fractal approach for the strength or hardness and for the fracture toughness are described by Eqs. (13) and (16) Accordingly, we can define a Fractal Structural Parameter (FSP) as

$$\text{FSP} = v^{\frac{\gamma}{2}} R^{\frac{3}{2}(\gamma-1)} d^{1-\frac{3}{2}\gamma} \tag{18}$$

for which:

$$\sigma_c^{\langle \text{grain} \rangle} \propto \text{FSP}. \tag{19}$$

Previous investigations on fragment size distributions [34] seem to suggest $\gamma = 2/3$ at small scale, as well as $\gamma = 1$ at large scale. These limit cases, together with their intermediate reference case, correspond respectively to:

$$\gamma = 2/3: \quad \mathrm{FSP} \propto v^{\frac{1}{3}} R^{-1/2} d^{0}, \tag{20a}$$

$$\gamma = 5/6: \quad \mathrm{FSP} \propto v^{\frac{5}{12}} R^{-1/4} d^{-1/4}, \tag{20b}$$

$$\gamma = 1: \quad \mathrm{FSP} \propto v^{\frac{1}{2}} R^{0} d^{-1/2}. \tag{20c}$$

Since $\sigma_C \propto k + \mathrm{FSP}$, Eqs. (20) indicate a deviation of the exponent in the Hall–Petch relationship of Eq. (4). It is interesting to observe that Masamura et al. [38] describe a similar deviation for the exponent of the Hall–Petch relationship. The experiments on fine grained micro- and nano-structured materials seem in fact to suggest three different regions for the exponent of the Hall–Petch relationship:

a region for single crystal to a grain size of about 1 μm, where the exponent seems to be close to 1/2.
a region for grain sizes ranging from about 1 μm to 30 nm, showing exponents lower than 1/2.
a region below a very small critical grain size (of about 30 nm), with the exponent equal to zero.

Note that, in this case, the reinforcement grain size effect is null, whereas the size-scale effect (i.e. the effect of the structural size R) is maximum.

Thus, it appears that the fractal approach is not only able to justify the empirical Hall–Petch law, but also to predict the deviation of its exponent. The inverse Hall–Petch behaviour (i.e. softening associated with grain refinement), experimentally observed by several Authors, may be interpreted in the present framework by using values of γ smaller than 2/3. In this case the dependency of strength on the grain size becomes positive, since the exponent $1 - (3/2)\gamma$ in Eq. (18) changes its sign.

On the other hand, it is clear that both scaling laws (Eqs. (13) and (16)) are monotonic laws, therefore not apt to describe a transition from the usual Hall–Petch behaviour to the anomalous, inverse one. Therefore, in the following assessment on experimental data, only monotonic data sets will be considered.

6. Experimental assessment of the FSP on WC–Co alloys and PCD

It has been already shown that the specimen size effects predicted by Eqs. (18) and (19) agree with the experiments satisfactorily (see [35]), so that we are herein more interested in the effects of grain size and volumetric content of grains. Eqs. (13) for strength (or hardness) may be rewritten as

$$y = \frac{(\sigma_c - (1-v)\sigma_c^{\langle \mathrm{matrix} \rangle}) R^{\frac{3}{2}}}{v d R^{\frac{3}{2}}} = k_\sigma \left(v^{\frac{1}{\gamma}} R^{\frac{3}{2}} d^{-\frac{3}{2}} \right)^{\gamma} = k_\sigma x^{\gamma}. \tag{21a}$$

Therefore, the fractal approach implies a power law between y and x with an exponent γ comprised between 2/3 and 1. This is equivalent to verify the validity of the FSP-based approach. The advantage here is that the exponent γ, as well as the constant of proportionality k_σ, can be easily obtained as best fit parameters.

When the material strength is predicted, then the fracture toughness can be also estimated by Eqs. (16):

$$y = \frac{(K_{IC} - (1-v)K_{IC}^{\langle \mathrm{matrix} \rangle}) R^{\frac{3}{2}}}{v^{1+\frac{\gamma}{2}} d^{\frac{3}{2}} R^{\frac{3}{2}}} = k_K k_\sigma \left(R^{\frac{3}{2}} d^{-\frac{3}{2}} \right)^{\gamma + \frac{2}{3}\alpha} = k_{K\sigma} x^{\gamma + \frac{2}{3}\alpha}, \tag{21b}$$

by fitting $k_{K\sigma}$, α.

We refer to the experimental investigation on fine grained PCD, reported by Lammer [39] and Huang et al. [40]. In addition, to assess the FSP on a larger data set, we also refer to the extensive experimental investigations on micro- and nano-grained WC–Co alloys available in the Literature [16,9,24,7,4,8,5,11,6,10,41,12].

In Fig. 1, the experimental assessment of the fractal theory according to Eq. (21) (assuming a unit specimen size; all the parameters are expressed in [SI] units), is presented for the strength and toughness of PCD. Data set [39] has been shifted vertically by unity for clarity reasons. Such experiments strongly confirm the prediction of the fractal approach. The exponents γ, which are the slopes in the strength diagrams, are found belonging to the theoretical range for each considered material.

In Fig. 2 the same analysis is carried out for the strength and toughness of WC–Co alloys, confirming the same findings. The reported data sets have been taken from: [4–6,8–10,12,15–17,20,24,41]. Also in this case the data sets have been shifted vertically by unity for clarity reasons. In each case, the agreement between FSP-based mixture rule and experiments is very good, as shown also by values of the regression parameter R^2. Three of these data sets are not complete and report hardness data only [15,16,20].

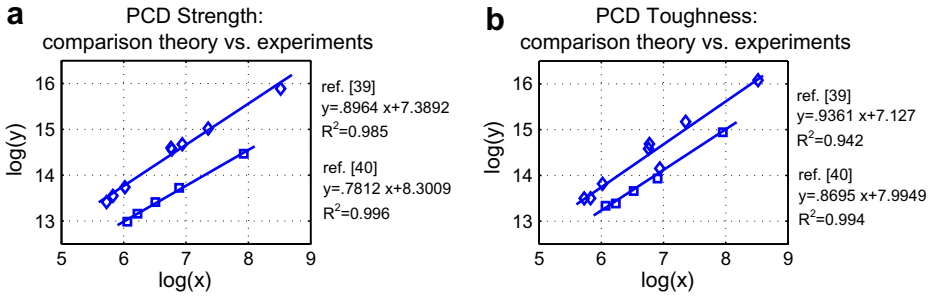

Fig. 1. PCD – Comparison between theory (straight line) and experiments (points): strength (a) and toughness (b). Data set [39] has been shifted vertically by unity for clarity reasons.

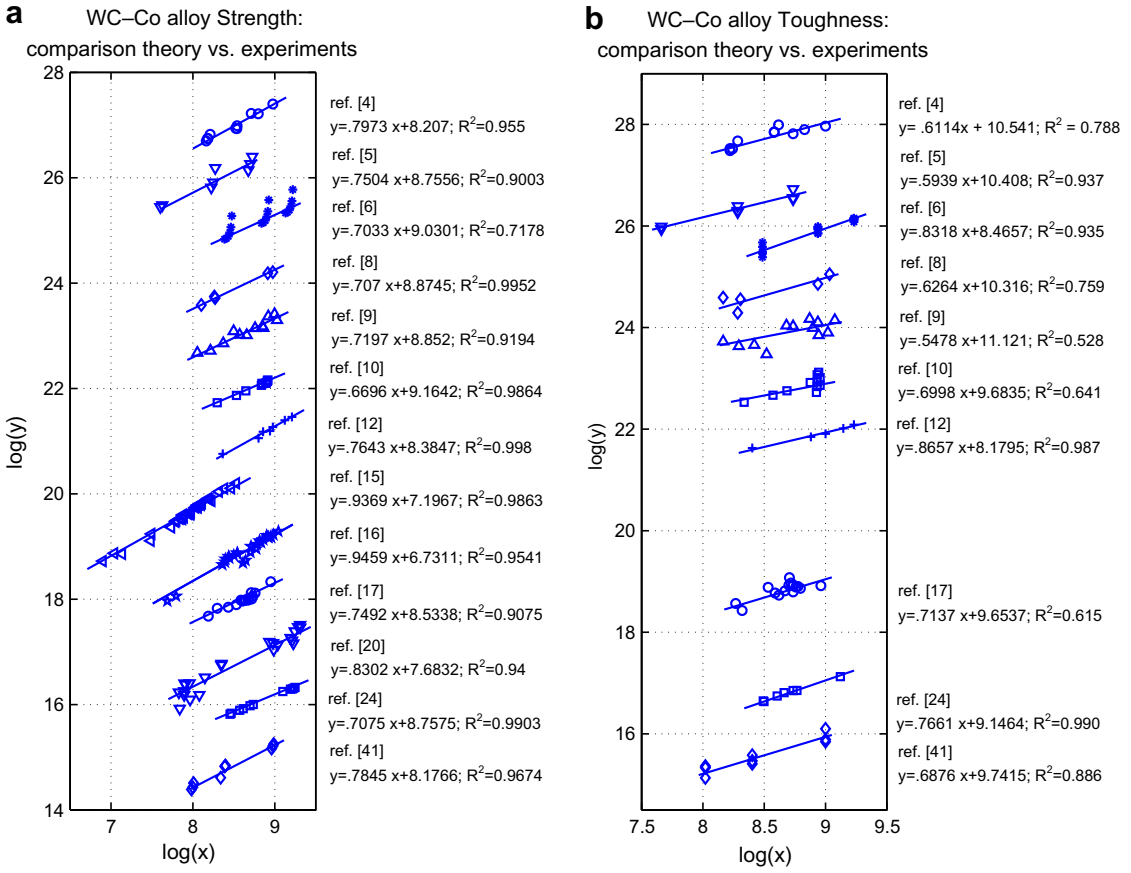

Fig. 2. WC–Co alloys – Comparison between theory (straight line) and experiments (points): strength (a) and toughness (b). Data relative to the inversion of the Hall–Petch law have been discarded and reported in Fig. 3. All data sets (except [41]) have been shifted vertically for clarity reasons.

It is worthwhile noting that the FSP-based mixture rules fit the experiments on hardness better than those on fracture toughness; this trend is particularly evident with the data sets by Nakamura and Gurland [9] and Sadahiro and Takatsu [10].

As already stated, both scaling laws (Eqs. (13) and (16)) are monotonic laws, therefore not apt to fit data describing a transition from the usual Hall–Petch behaviour to the anomalous, inverse one. As a consequence, only data sets

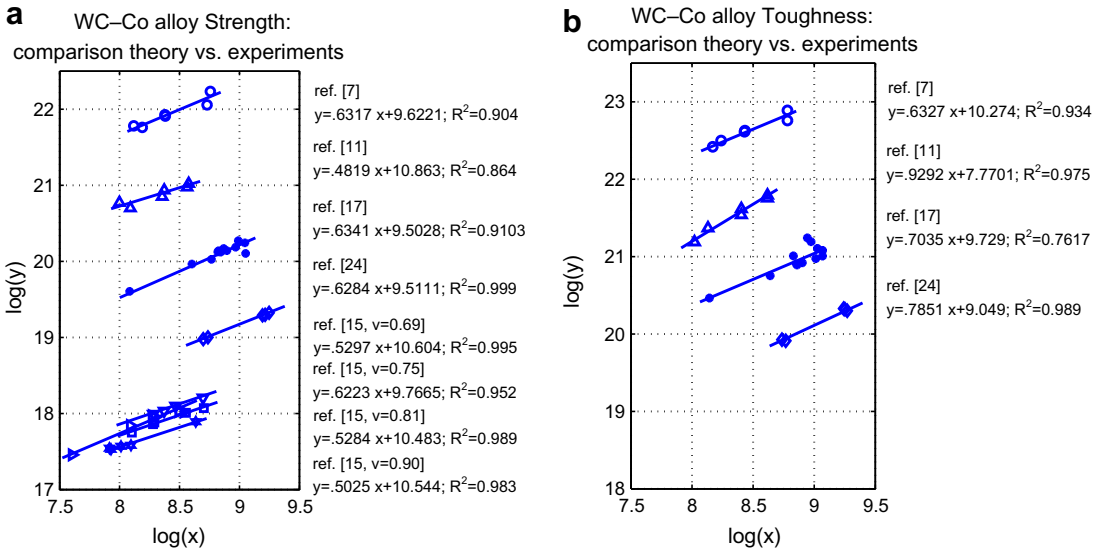

Fig. 3. WC–Co alloys – Comparison between theory (straight line) and experiments (points): strength (a) and toughness (b). Data relative to the inversion of the Hall–Petch law only. All data sets (except [15]) have been shifted vertically for clarity reasons.

displaying a monotonic trend in hardness (or strength) vs. grain size d have been fitted. In the case of data sets displaying both Hall–Petch ranges [15,17,24], data relative to the inverse Hall–Petch behaviour have been discarded and then fitted separately in Fig. 3, together with two more data sets [7,11], which display the inverse Hall–Petch behaviour only. Once again, different data sets have been shifted vertically by unity for clarity reasons.

Also in this case the agreement between the proposed approach and the experiments is remarkably good. It is worthwhile noting that the inverse Hall–Petch behaviour is described consistently by a γ exponent falling outside the canonical range, i.e., lower than 2/3 (see Fig. 3a). In the case of the data set by Gurland [16], however, it results that the effect of composition v is not captured by the FSP (see Fig. 3a). In other words, data do not collapse onto the same line and different values of v arrange themselves on different lines.

We also notice that, with these data sets, the FSP-based mixture rules fit the data of fracture toughness better than those of hardness, in contrast to what happened with the previous data sets. Regarding toughness, if we consider the data sets by Sigl and Fischmeister [24] and Pickens and Gurland [17], which display both Hall–Petch ranges, it may be noted that the slope in the toughness diagram does not change significantly (compare Fig. 2b with Fig. 3b).

Summarizing, the FSP of Eq. (18) represents an important tool to predict grain size effects, as well as the influence of the volumetric grain content, for micro- and nano-grained materials. In addition, the FSP may also describe the influence of the structural size on material properties.

7. Material design and optimization

From the FSP-based laws (Eqs. (13) and (16)), strength and toughness can be derived as functions of volumetric grain content, grain size and structural dimension. According to the FSP-based laws in which the constant of proportionality and the exponents are fitted from the experiments by Huang et al. [40], the following laws for PCD (in [SI]) are found:

$$\sigma_c(d,v) \approx (1-v)\sigma_c^{\langle \text{matrix} \rangle} + 200 \times 10^6 \times v^{1.391} d^{-0.172}, \tag{22a}$$

$$K_{IC}(d,v) \approx (1-v)K_{IC}^{\langle \text{matrix} \rangle} + 99 \times 10^6 \times v^{1.391} d^{0.196}, \tag{22b}$$

with $\sigma_c^{\langle \text{matrix} \rangle} \approx 500$ MPa, $K_{IC}^{\langle \text{matrix} \rangle} \approx 20$ MPa$\sqrt{\text{m}}$. The structural dimension R is here neglected (and fictitiously assumed to be equal to the unity in [SI]) as a consequence of the identical sizes for the investigated specimens. In addition, considering a reference PCD with grain size d_r and volumetric content v_r, we can deduce the increments in strength (or hardness $H \propto \sigma_c$) and fracture toughness expected by using a new PCD material, designed with different grain size d and volumetric content v. For example, for the hardness we would have to evaluate the ratio

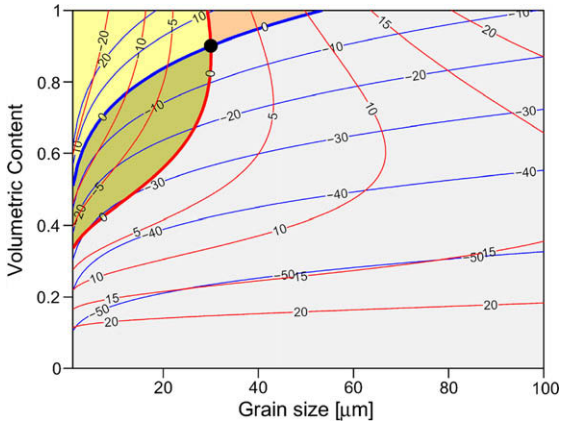

Fig. 4. PCD optimization map. Iso-hardness lines are drawn in blue and iso-toughness lines in red. Numbers along the curves indicate hardness and fracture toughness increments % [40].

$[H(d,v)-H(d_r,v_r)]/H(d_r,v_r)\cdot 100\%$. In Fig. 4, the increments of the hardness and of the fracture toughness for a standard PCD ($v_r \approx 0.9$, $d_r \approx 30$ μm, $\sigma_c^{\langle matrix\rangle} \approx 500$ MPa, $K_{IC}^{\langle matrix\rangle} \approx 20$ MPa$\sqrt{m}$) are reported. The experimental range for the grain size is from 5 to 90 μm, whilst that for the volumetric content is from 0.89 to 0.95; thus, large part of the graph is, strictly speaking, an extrapolation. This diagram can be considered as a PCD optimization map. Note the small (orange) region where both the increments are positive: a new PCD belonging to this region will be harder and tougher at the same time (with respect to the reference one). Basically, the increment in hardness is given by the increase in the volume fraction of hard phase, which counterbalances the increase in d. The increment in fracture toughness, on the other hand, is given by the rising of the grain size d, which counterbalances the decrease of the ductile phase volume fraction.

The same operation has been performed also in the case of the WC–Co alloy. According to the FSP-based laws in which the constant of proportionality and the exponents are fitted from the experiments on nano-structured alloys created by Jia et al. [12], the following laws (in [SI]) are found:

$$\sigma_c(d,v) \approx (1-v)\sigma_c^{\langle matrix\rangle} + 242\times 10^6 \times v^{1.382} d^{-0.146}, \tag{23a}$$

$$K_{IC}(d,v) \approx (1-v)K_{IC}^{\langle matrix\rangle} + 151\times 10^6 \times v^{1.382} d^{0.201}, \tag{23b}$$

with $\sigma_c^{\langle matrix\rangle} \approx 500$ MPa, $K_{IC}^{\langle matrix\rangle} \approx 20$ MPa$\sqrt{m}$. The structural dimension R is again neglected (and fictitiously assumed to be equal to the unity in [SI]), since all specimens come from the same data set [12]. Considering a reference alloy with grain size d_r and volumetric content v_r, we can deduce the increments in strength (or hardness $H \propto \sigma_c$) and fracture toughness expected by using a new WC–Co material, designed with different grain size d and volumetric content v.

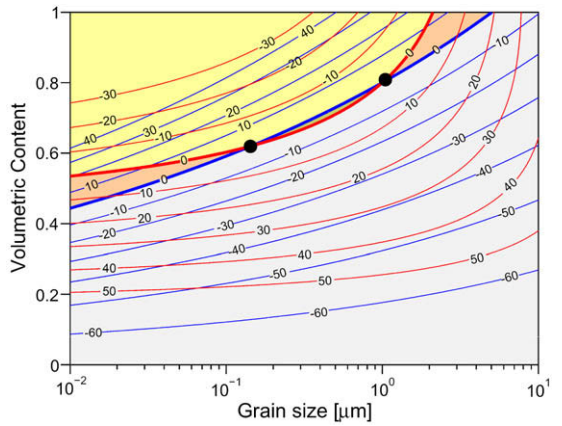

Fig. 5. WC–Co alloy optimization map. Iso-hardness lines are drawn in blue and iso-toughness lines in red. Numbers along the curves indicate hardness and fracture toughness increments % [12].

In Fig. 5, the increments of the hardness and of the fracture toughness for a reference WC–Co Alloy ($v_r \approx 0.8$, $d_r \approx 2$ μm, $\sigma_c^{\langle matrix \rangle} \approx 500$ MPa, $K_{IC}^{\langle matrix \rangle} \approx 20$ MPa$\sqrt{m}$) are reported. This diagram may be considered as a WC–Co alloy optimization map. In this case, the experimental range for the grain size is from 70 nm to 2.5 μm, whilst that for the volumetric content is from 0.69 to 0.90.

In comparison with the previous case, where the range for the grain size d did not extend below 1 μm, the difference is given by the presence of two regions (marked in orange) where both the increments are positive. One of them is similar to that in Fig. 4: in fact, it is characterized by a simultaneous increase in both d and v. The second region, which extends itself towards the left, i.e. towards nano-sized grains, is characterized by a simultaneous decrease in both d and v. Thus, the mechanisms which produce better material properties are opposite to those operating in the other region. The hardness increases thanks to the decrease in the grain size, which counterbalances the decrease in the volume fraction v of hard phase. On the other hand, fracture toughness increases, despite the grain size decrease, thanks to the increase in the ductile phase volume fraction. This remark suggests that better nano-grained composites should be produced by coupling nano-sized grains with volume percentages smaller than those usually employed in conventional micro-grained alloys.

8. Conclusions

A generalization of the Hall–Petch law for grain size effect on material strength, $\sigma_C \propto k + d^{-1/2}$, was introduced by Gurland [15], as $\sigma_c \propto k + v^{\frac{1}{3}} d^{-\frac{1}{2}}$, to take into account the volumetric grain content. Our approach represents a further generalization of the Gurland's parameter, introducing a fractal structural parameter (FSP), in which the scaling related to the structural dimension R is also included and in which the fractal exponents are generalized, i.e., $\sigma_C \propto k + v^{\frac{\gamma}{2}} R^{\frac{3}{2}(\gamma-1)} d^{1-\frac{3}{2}\gamma}$.

The fractal approach seems to present at the same time the fascinating advantages of incorporating the classical approach with different types of grain size distributions (e.g., the Gaussian and the Log-normal), the influence of the composition, as well as reasonable grain and structural size-effects. In addition, it provides hints for the design of conventional, as well as nano-structured brittle materials reinforced with a ductile phase. For these reasons, and in virtue of a very broad successful assessment with experimental data from the Literature, the Fractal Structural Parameter (FSP) could help in designing optimized innovative micro- and nano-structured materials.

Acknowledgements

The financial support of the European Union to the Leonardo da Vinci Project I/06/B/F/PP-154069 "Innovative Learning and Training on Fracture (ILTOF)" is gratefully acknowledged.

Appendix A. The role of contiguity and mean free path

Let contiguity C_i be defined for a given phase i. We can extend the concept defining the contiguity C_{ij} of the phase i with respect to the phase j as *the average fraction of surface area shared by the grains of the phase i with all neigh-boring particles of the phase j*.

According to such definition, an estimation of the contiguity can be obtained assuming that the shared surface area between the two phases i and j, S_{ij}, is statistically proportional to the product of their total surface areas S_i, S_j:

$$C_{ij} = \frac{S_{ij}}{S_i} \propto \frac{S_i S_j}{S_i} = S_j. \tag{24}$$

From Eq. (6), noting that $S_g \approx W \approx W_C V$, the relation between surface and volume is $S \approx V^{\gamma}$ ($\gamma \approx D/3$), or for a given phase j:

$$S_j \propto V_j^{\gamma_j}, \tag{25}$$

so that Eq. (24) becomes:

$$C_{ij} \propto V_j^{\gamma_j}. \tag{26}$$

Considering that $C_i \equiv C_{ii}$ and assuming $\gamma_i = \gamma$:

$$C_i = v_i^{\gamma}. \tag{27}$$

In the fractal approach, the contiguity effect is simply equivalent to consider a different power of the volumetric fraction of the phase. In other words, in the fractal approach the parameter γ plays the key role, since also the contiguity is not an independent parameter. It is interesting to observe that, according to Eqs. (3) and (27), the classical direct rule of mixture of Eqs. (1) and (2) for the generic property P, may be rewritten as

$$P = \sum_{i=1}^{N} P_i v_i^{1+\gamma} \tag{28}$$

and is close to the empirical rule of mixture in which the volumetric fraction is raised to the exponent 2, obtained as a limit case for $\gamma = 1$. Accordingly, the fractal approach provides the reason for the exponent 2 in the empirical mixture rule, which is often used in order to have a better description of the experimental data [42].

Regarding the mean free path h, it could be shown that it is a function of the mean grain size d and of the volumetric fraction of grains v, if a regular arrangement of grains is assumed. For instance, by assuming a tetrakaidecahedra shape for the grains, [43]. provided a simple formula relating these three quantities:

$$v = \frac{(d-h)^3}{d^3}, \tag{29}$$

In the case of more realistic distribution of grains, with dispersion of grain size d, it has been shown by means of stereology [44]. that h depends not only on d and v, but also on the contiguity C:

$$h = d\frac{(1-v)}{v(1-C)}. \tag{30}$$

Since the contiguity C itself depends on v and d (see Eq. (27) or the relations proposed by Golovchan and Litoshenko [23], it is clear that h also depends on these two variables.

Appendix B. The Gaussian and the Log-normal distributions

From the fractal approach, the scaling of the energy density has been obtained as reported in Eq. (12). In this appendix we show how such a result is more general than expected. In particular, we show that, assuming a Gaussian distribution for the grain sizes, the energy density scales as predicted by the fractal approach in the limit case of $\gamma = 1$. Let us assume a Gaussian (or normal) distribution of grains, for which the probability density function $p(r)$ is

$$p(r) = \frac{1}{\sqrt{2\pi}\sigma}\exp\left[-\frac{(r-r_m)^2}{2\sigma^2}\right], \tag{31}$$

where σ is the standard deviation and r_m is the mean grain size, i.e.:

$$\langle r\rangle \propto \frac{1}{N_0}\int_0^\infty r\mathrm{d}N \propto \int_{-\infty}^{\infty} rp(r)\mathrm{d}r = r_m. \tag{32}$$

Note that the integrals evaluated between minus infinite and zero must give negligible contributions to the final results, the variable r being defined as positive. The energy dissipation W connected to the presence of the grains is statistically expected to be proportional to their total surface area, i.e.:

$$W \propto S_g \propto \int_0^\infty r^2\mathrm{d}N = \int_0^\infty N_0 r^2 p(r)\mathrm{d}r = N_0(r_m^2+\sigma^2). \tag{33}$$

On the other hand, the total volume of the grains is

$$V_g \propto \int_0^\infty r^3\mathrm{d}N \propto \int_0^\infty N_0 r^3 p(r)\mathrm{d}r = N_0(r_m^3+3r_m\sigma^2). \tag{34}$$

Deriving the expression of N_0 from the previous equation and introducing it into Eq. (33), being $r_m \approx d$, yields the asymptotic behaviour:

$$W \propto V_g d^{-1} \propto vd^{-1}, \tag{35}$$

identical to Eq. (12) if $\gamma = 1$. The same result is provided if we consider a Log-normal distribution, for which the probability density function $p(r)$ is

$$p(r) = \frac{1}{r\sqrt{2\pi}S}\exp\left[-\frac{(\ln(r)-M)^2}{2S^2}\right], \tag{36}$$

where M is the scale parameter and $S \geqslant 0$ the shape parameter. The mean grain size r_m and the standard deviation σ are given by

$$r_m = \int_{-\infty}^{\infty} rp(r)\mathrm{d}r = \exp\left[M + \frac{S^2}{2}\right], \tag{37}$$

$$\sigma^2 = \int_{-\infty}^{\infty} (r - r_m)^2 p(r)\mathrm{d}r = \exp(2M + S^2)[\exp(S^2) - 1]. \tag{38}$$

As in the previous case, the energy dissipation W connected to the presence of the grains is statistically expected to be proportional to their total surface area, i.e.:

$$W \propto S_g \propto \int_0^{\infty} r^2 \mathrm{d}N = \int_0^{\infty} N_0 r^2 p(r)\mathrm{d}r = N_0 \exp[2(M + S^2)]. \tag{39}$$

On the other hand, the total volume of the grains is

$$V_g \propto \int_0^{\infty} r^3 \mathrm{d}N \propto \int_0^{\infty} N_0 r^3 p(r)\mathrm{d}r = N_0 \exp\left[3M + \frac{9}{2}S^2\right]. \tag{40}$$

Deriving the expression of N_0 from the previous equation and introducing it into Eq. (39), being $r_m \approx d$, yields the asymptotic behaviour:

$$W \propto V_g \exp\left[-\left(M + \frac{5}{2}S^2\right)\right] \propto v\frac{1}{d}\left(\frac{d^2}{d^2 + \sigma^2}\right)^2 \propto vd^{-1}, \tag{41}$$

which is identical to Eq. (12) if, again, $\gamma = 1$.

Appendix C. Agreement with fragmentation theory

The scaling law of the additional energy density dissipated as a consequence of the presence of the grains and interfaces, Eq. (12), may be interpreted with findings by [33–35] from fragmentation theories. In a fragmentation process of a mixture of total volume V, with phases of volumes V_i, the total dissipated energy W can be evaluated as

$$W = \sum_{i=1}^{N} W_i = \sum_{i=1}^{N} \Gamma_i V_i^{\gamma_i} = \Gamma V^{\gamma}, \tag{42}$$

where $\gamma_i = 2/3$ to 1 are the fractal exponents and Γ_i are material constants of the phases (the so-called *fractal fragmentation strengths*). The parameters γ and Γ represent the fractal exponent and fragmentation strength of the mixture. The constants Γ_i are by definition the size-independent mechanical properties of the materials. For the particular case of $\gamma_i = \gamma$:

$$\Gamma = \sum_{i=1}^{N} \Gamma_i v_i^{\gamma}, \tag{43}$$

where $v_i = V_i/V$ is the volumetric fraction of the phase i. The exponent $\gamma = 2/3$ describes a rule of mixture governed by the surfaces of the components, as well as the exponent $\gamma = 1$ represents, as a limit case, the classical approach describing volume dominated processes. Eqs. (42) and (43) are consequences of the universal laws derived in the evaluation of the multiscale energy dissipation during fragmentation and comminution [33]. Eq. (43) shows that fractal mechanical properties, rather than the classical ones, should be considered as the real properties of the phases and of the mixture. Comparing Eqs. (12) and (42) yields the dependence of the material property on the grain size:

$$\Gamma \propto d^{2-3\gamma}. \tag{44}$$

This equation, for multi-phase materials, would have to be applied to each phase i, yielding:

$$\Gamma_i \propto d_i^{2-3\gamma_i}. \tag{45}$$

Assuming $\gamma_i = \gamma$ and introducing Eq. (45) into Eq. (43) yields:

$$\Gamma = \sum_{i=1}^{N} k_i d_i^{2-3\gamma} v_i^{\gamma}, \tag{46}$$

where k_i is a constant related to the phase i. Eq. (46) represents the fractal size-independent specific energy dissipation, in agreement with Eq. (12).

References

[1] Chermant JL. Les céramiques thermomécaniques. Paris: Les Presses du CNRS; 1989.
[2] Tenckhoff E, Vöhringer O. Microstructure and mechanical properties of materials. Oberursel: DGM Informationsgesellschaft Verlag; 1990.
[3] Rice RW. Mechanical properties of ceramics and composites. New York: Marcel Dekker; 2000.
[4] Ingelstrom N, Nordberg H. The fracture toughness of cemented tungsten carbides. Eng Fract Mech 1974;6:597–607.
[5] Lueth RC. Determination of fracture toughness parameters for tungsten carbide–cobalt alloys. In: Bradt RC et al., editors. Fracture mechanics of ceramics. New York: Plenum; 1974. p. 791–806.
[6] Chermant JL, Ostertock F. Fracture toughness and fracture of WC–Co composites. J Mater Sci 1976;11:1939–51.
[7] Murray MJ. Fracture of WC–Co alloys: an example of spatially constrained crack tip opening displacements. Proc Roy Soc Lond A 1977;356:483–508.
[8] Lindau L. In: Taplin DMR, editor. Fracture 1977, advances in research on the strength and fracture of materials. In: Proceedings of the 4th international conference on fracture, vol 2. 1977. p. 215–22.
[9] Nakamura M, Gurland J. The fracture toughness of WC–Co two-phase alloys – a preliminary model. Metall Trans A 1980;11:141–6.
[10] Sadahiro T, Takatsu S. A new pre-cracking method for fracture toughness testing of cemented carbides. Mod Dev Powder Metall 1980;14:561–72.
[11] Viswanatham RK, Sun TS, Drake EF, Peck JA. Quantitative fractography of WC–Co cermets by auger spectroscopy. J Mater Sci 1981;16:1029–38.
[12] Jia K, Fischer TE, Gallois B. Microstructure, hardness, and toughness of nanostructures and conventional WC–Co composites. Nanostruct Mater 1998;10:875–91.
[13] Richter V, von Ruthendorf M. On hardness and toughness of ultrafine and nanocrystalline hard materials. Int J Refract Met Hard Mater 1999;17:141–52.
[14] Milman YV, Luyckx S, Goncharuck VA, Northrop JT. Results from bending tests on submicron and micron WC–Co grades at elevated temperatures. Int J Refract Met Hard Mater 2002;20:71–9.
[15] Gurland J. The fracture strength of sintered tungsten carbide–cobalt alloys in relation to composition and particle spacing. Trans Metall Soc AIME 1963;227:1146–50.
[16] Lee HC, Gurland J. Hardness and deformation of cemented tungsten carbide. Mater Sci Eng 1978;33:125–33.
[17] Pickens JR, Gurland J. The fracture toughness of WC–Co alloys measured on single-edge notched-beam specimens precracked by electron-discharge machining. Mater Sci Eng 1978;33:135–42.
[18] Ravichandran KS. A survey of toughness in ductile phase composites. Scr Metall Mater 1992;26:1389–93.
[19] Ravichandran KS. Fracture toughness of two phase WC–Co CerMets. Acta Metall Mater 1994;42:140–3.
[20] Makhele-Lekala L, Luyckx S, Nabarro FRN. Semi-empirical relationship between the hardness, grain size and mean free path of WC–Co. Int J Refract Met Hard Mater 2001;19:245–9.
[21] Armstrong RW, Cazacu O. Indentation fracture mechanics toughness dependence on grain size and crack size: application to alumina and WC–Co. Int J Refract Met Hard Mater 2006;24:129–34.
[22] Liu B, Zhang Y, Ouyang S. Study on the relation between structural parameters and fracture strength of WC–Co cemented carbides. Mater Chem Phys 2000;62:35–43.
[23] Golovchan VT, Litoshenko NV. On the contiguity of carbide phase in WC–Co hardmetals. Int J Refract Met Hard Mater 2003;21:241–4.
[24] Sigl LS, Fischmeister HF. On the fracture toughness of cemented carbides. Acta Metall 1988;36:887–97.
[25] Carpinteri A, Pugno N. Strength and toughness of micro- and nano-structured materials: unified influence of composition, grain size and structural dimension. Rev Adv Mater Sci 2005;10:320–4.
[26] Carpinteri A, Pugno N. Are scaling laws on strength of solids related to mechanics or to geometry? Nature Mater 2005;4: 421–3.
[27] Dvorak GJ, Srinivas MV. Transformation field analysis of damage evolution in composite materials. J Mech Phys Solids 1999;47:899–920.
[28] Dvorak GJ, Srinivas MV. New estimates of overall properties of heterogeneous solids. J Mech Phys Solids 2001;49:2517–41.
[29] Hall EO. The deformation and ageing of mild steel: III Discussion of results. Proc Phys Soc B 1951;64:747–53.
[30] Petch NJ. The cleavage strength of polycrystals. J Iron Steel Inst 1953;174:25–8.
[31] Carpinteri A. Fractal nature of material microstructure and size effects on apparent mechanical properties. Mech Mater 1994;18:89–101.
[32] Carpinteri A. Scaling laws and renormalization groups for strength and toughness of disordered materials. Int J Solids Struct 1994;31:291–302.
[33] Carpinteri A, Pugno N. A fractal comminution approach to evaluate the drilling energy dissipation. Int J Numer Anal Methods Geomech 2002;26:499–513.

[34] Carpinteri A, Pugno N. One-, two- and three-dimensional universal laws for fragmentation due to impact and explosion. J Appl Mech 2002;69:854–6.
[35] Carpinteri A, Pugno N. Scale-effects on mean and standard deviation of the mechanical properties of condensed matter: an energy-based unified approach. Int J Fract 2004;128:253–61.
[36] Carpinteri A, Cornetti P, Puzzi S. A stereological analysis of aggregate grading and size effect on concrete tensile strength. Int J Fract 2004;128:233–42.
[37] Carpinteri A, Cornetti P, Puzzi S. Scale effects on strength and toughness of grained materials: an extreme value theory approach. Strength Fracture Complex 2005;3:175–88.
[38] Masamura RA, Hazzledine PM, Pande CS. Yield stress of fine grained materials. Acta Mater 1998;46:4527–34.
[39] Lammer A. Mechanical properties of polycrystalline diamonds. Mater Sci Technol 1998;4:949–55.
[40] Huang B-L, Weis C, Yao X, Belnap D, Rai G. Fracture toughness of sintered polycrystalline diamond (PCD). In: Froes FH, Hebeisen JC, editors. Proceedings of the 5th international conference on advanced particulate materials & processes. Princeton (NJ): Metal Powder Industries Federation; 1997. p. 431–7.
[41] Scussel HJ. Friction and wear of cemented carbides. In: Friction, lubrication and wear technology. ASM handbook, vol. 18. ASM International; 1992. p. 795–800.
[42] Zum-Gahr KH. Microstructure and wear of materials. Tribology Series, vol. 10, Elsevier; 1987.
[43] Palumbo G, Thorpe SJ, Aust KT. On the contribution of triple junctions to the structure and properities of nanocrystalline materials. Scripta Metall Mater 1990;24:1347–50.
[44] Underwood EE. Quantitative stereology. Cambridge Massachusetts: Addison-Wesley; 1970.